

Groundwater evolution, authigenic carbonates and sulphates, of the Basque Lake No. 2 Basin, Canada

H. WAYNE NESBITT

Department of Geology, University of Western Ontario, London, Ontario N6A 5B7, Canada

Abstract—The Basque Valley includes four drainage basins each a few hundreds of metres long and 100 to 200 metres wide. The major aquifer of Basque #2 basin is a thin horizon of Mazama Ash (Crater Lake, 6000 years old). The present hydrological and geochemical regime has developed since deposition of the ash.

Waters of the Basque Lake #2 basin are concentrated more than 100 fold to produce the Mg-SO₄-rich brines. During the first 10-fold concentration Mg-calcite (8 to 29 mole percent MgCO₃), and protodolomite (32 to 43 mole percent MgCO₃) are precipitated sequentially from the progressively more concentrated waters. Magnesite and the sulphate salts, gypsum, epsomite (MgSO₄ · 7H₂O) and bloedite (Na₂Mg(SO₄)₂ · 4H₂O) are precipitated during the second 10-fold concentration. Precipitation of Mg-calcite dramatically increases Mg/Ca of the basin waters during concentration as does formation of protodolomite. Continued concentration, with precipitation of gypsum and magnesite yields Mg-SO₄-rich, and Ca-CO₃-depleted brines from which epsomite and bloedite precipitate.

Mg-calcite and groundwater compositions yield exchange constants similar to experimental values, demonstrating that exchange equilibrium is achieved between solution and calcite in the basin. The result supports application of exchange equilibrium concepts to carbonate authigenesis in natural settings. A thermodynamic model provides a simple explanation for the evolution of the waters of the Basque and Spotted Lake Basins, and has implications for the evolution of seawater concentrates in diagenetic environments.

Aqueous silica concentrations diminish whereas Al(aq) increases in the progressively more concentrated waters. X-ray diffraction studies of the fine grained silicate fraction demonstrate that extensive reaction has occurred between the Basque waters and the phyllosilicates of the muds.

INTRODUCTION

SMALL CLOSED DRAINAGE BASINS are excellent natural laboratories in which to study interactions between natural solutions and minerals (GARRELS and MACKENZIE, 1967; JONES, 1966; HARDIE, 1968; EUGSTER, 1969, 1970; HARDIE and EUGSTER, 1970; JONES *et al.*, 1977; DROUBI *et al.*, 1977; GAC *et al.*, 1977). These studies also emphasize the deficiencies in our knowledge and understanding of natural processes. For example, very early in the study of these basins HARDIE and EUGSTER (1970) commented that the behaviour of Mg was both poorly documented and understood. They suggested a study of brines rich in Mg, with emphasis placed on the behaviour of Mg. The results are presented here. Numerous studies directed towards the behaviour of Mg have been conducted subsequently (DREVER, 1971; NESBITT, 1975; GAC *et al.*, 1977). This study documents the effects of carbonate formation on the behaviour of Mg in the Basque No. 2 basin.

The carbonates represent a potentially large sink for Mg, particularly Mg-calcites (GOLDSMITH *et al.*, 1955) and Ca-protodolomites (SKINNER, 1963). There are many reports that note the formation of these phases in natural settings (ALDERMAN and

SKINNER, 1957; SKINNER, 1963; VON DER BORSCH, 1965; GLOVER and PRAY, 1969; BARNES and O'NEIL, 1971; MULLER *et al.*, 1972; MUCCI *et al.*, 1985; ROSEN and WARREN, 1988; ROSEN *et al.*, 1989). Only recently, however, have interactions between Mg(aq) and carbonates been understood in detail (MUCCI and MORSE, 1984, 1985). The compositional variations of the Mg-rich Basque Lake Basin waters, and properties of the associated authigenic minerals, are documented here and interpreted in the framework of these new findings. The results are combined with the recent experimental data to develop a simple geochemical model to explain both the evolution of the Basque Lake Basin ground waters and the production of associated authigenic carbonate-sulphate mineral zones. Some implications for the subsurface evaporative concentration of seawater are that Mg-calcite precipitation and decay of organics may affect early diagenetic nature and production of Mg-bearing carbonates and sulphates.

THE BASQUE NO. 2 BASIN

Introduction

The Basque Lakes contain the highest magnesium concentrations of known North American

closed basins (GOUDGE, 1924). The Lakes are situated in south-central British Columbia (Fig. 1), 100 km west of Kamloops (see GOUDGE, 1924 for details). The Basque Valley contains four small closed drainage basins separated by natural clay dams. The climate is arid, averaging 25 to 30 cm of rainfall annually and the temperature fluctuates seasonally, averaging -10°C in January and 25°C to 30°C during July and August. GOUDGE (1924) provides a detailed description of the Basque Valley so that additional description is restricted to the Basque No. 2 Basin.

Description

Basque No. 2 Basin (Fig. 1B) is approximately 800 m by 200 m with a small lake at its southern end (Fig. 2A). Standing water is found in the lake after spring runoff but by late summer evaporation has produced a salt crust on top of circular brine pools. The pools are surface expressions of conical structures (Fig. 2B) with springs at the centre of the cones (GOUDGE, 1924). Once the crust has formed, communication between the brine and atmosphere is through a small 5 to 10 cm circular hole in each salt crust. Brine remains below the crust during the driest periods and is replenished by the 'conical springs' (GOUDGE, 1924). Springs are absent from the perimeter of the lake and from the basin, except for those within the brine pools. There is no sig-

nificant surface runoff to the lake during the summer months. A detailed description is given by GOUDGE (1924).

Bedrock of volcanic and metamorphic origin crops out on the eastern and western flanks of the basin (Fig. 2B). A highly porous, permeable sand apron flanks the central valley floor (Fig. 2B), and is composed mainly of rock fragments, quartz and feldspar. No detrital carbonates were observed. Sands on the flanks of the valley give way to non-porous, highly impermeable muds of the valley floor (Fig. 2B). Attempts to collect water samples from these muds have been unsuccessful. Sandy lenses are scarce and no continuous horizons have been observed to date (upper 2 meters of sediment). Quartz and feldspar are abundant and a 10 \AA mica and 14 \AA chlorite dominate the less than $2\text{ }\mu$ fraction (Fig. 3B). Carbonates are absent from all muds *except those contacted by lake brines or ground waters of the basin*.

A highly porous, permeable volcanic ash horizon is present at $\frac{1}{2}$ m to 1.5 m depth (Fig. 2B). Grass rootlets penetrate the muds to the volcanic ash horizon. The grasses thrive on the basin floor during the dry summer months, whereas the sparse grasses outside the basin die. The ash is a source of water. Very thin discontinuous sandy lenses were found occasionally 0.2 m to 0.5 m below the ash. Authigenic carbonate minerals are found within the volcanic ash horizon but they are much more abundant

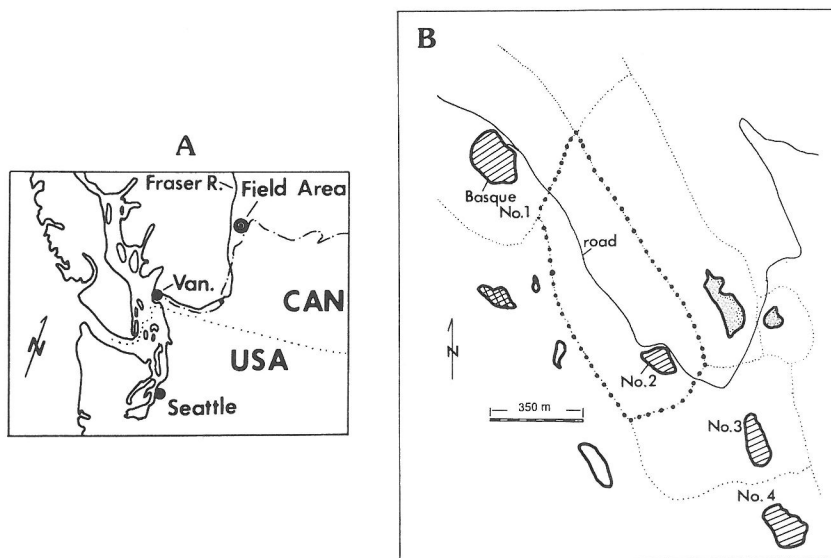


FIG. 1. Fig. 1A is a location of the Basque Lake Basin. The scale is 200 km. Fig. 1B is a plan view of the Basque Lake Basin showing the locations of the Basque Lakes (No. 1 to No. 4). The cross-hatched lake contains Na_2SO_4 brines and the stippled lakes contain Mg-carbonate salts.

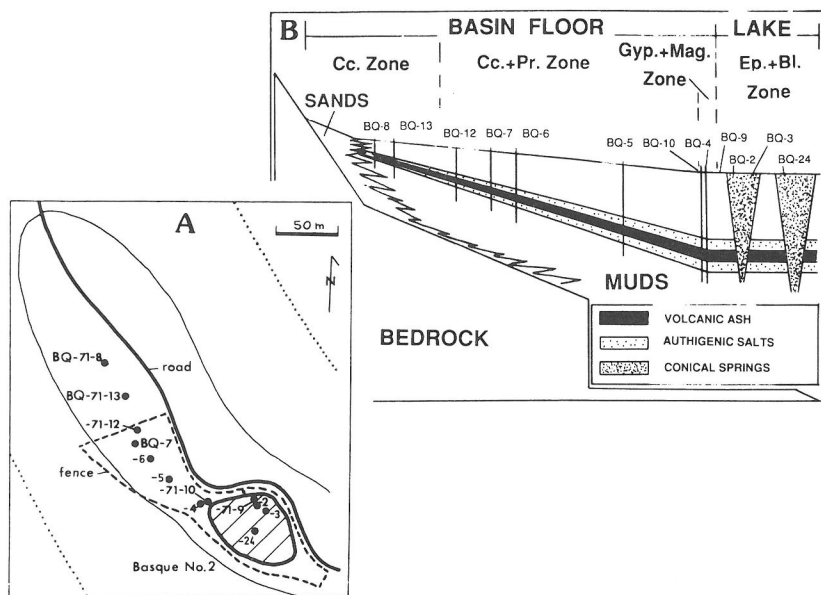


FIG. 2. Fig. 2A is a plan view of Basque Lake #2 Basin. The scale is 100 m. The hashed area is the lake proper and the dotted lines represent the margins of the basin. Dots represent sample locations. Sample labels are composed of a prefix 'BQ', a middle portion '70' or '71', (year sample was collected), and a suffix '8' (sample number). The prefix and '70' are omitted from some labels for clarity. The year, '70' and '71', is removed from labels in the text for brevity. Fig. 2B is a conceptualized cross-section showing the lake, and valley floor. Sample locations and mineral zones are included. Cc = calcite; Pr = protodolomite; Gyp = gypsum; Mag = magnesite; Ep = epsomite; Bl = bloedite.

in the muds immediately adjacent to the ash. Phyllosilicates of these muds are different from muds found well removed from the aquifer (Fig. 3A). Apparently they are altered from their original state to yield properties similar to those found in the lake muds (Fig. 3B). Immediately north of the lake at BQ-4, the ash is 10 to 15 cm thick and 1 m below ground surface. Further removed from the lake, near the head of the basin (Fig. 1B, BQ-13), the aquifer is 5 cm thick and 0.7 m below the ground surface. It thins and is found at shallower depths away from the lake. The aquifer is not exposed on the valley floor or around the perimeter of the basin. It is charged with solution in late July and where penetrated during coring, the holes filled rapidly with water from the aquifer.

Muds of the lake are different from other muds of the valley. Lake oozes are black, smell of H_2S , and contain authigenic carbonate minerals, sulphate minerals, chlorite and mica. There is no evidence that they have a different origin from the other muds, hence the difference in properties most likely result from reaction with the lake brines. Chlorite and mica, for example, display poorly defined peaks (Fig. 3B) compared with the peaks of Fig. 3A, and broad shoulders are found on the low 2θ side of

these peaks. The less than 2μ fraction is difficult to identify by X-ray diffraction methods (Fig. 3B). Ooze contacted by the brines are saturated but have very low permeability. Mud around the perimeter of the lake, between the spring high water mark and the low water mark of late summer have also been affected by contact with lake waters and brines and contain carbonate and sulphate salts.

Hydrological aspects

The volcanic ash aquifer is confined above and below by impermeable muds, does not outcrop (Fig. 2B), remains charged with water and retains a head during much of the summer period. The head is above the brine surface of the lake. Since the aquifer does not outcrop, it is not recharged directly by spring runoff. The sand apron on the flanks of the basin is sufficiently elevated and permeable to act as a reservoir. It is recharged each year by spring runoff and the volcanic ash aquifer may be hydrologically connected to the elevated unconfined sandy reservoir, as shown in Fig. 2B. The reservoir is large compared with the volume of the aquifer, thus providing sufficient capacity to replenish the aquifer into the dry summer period.

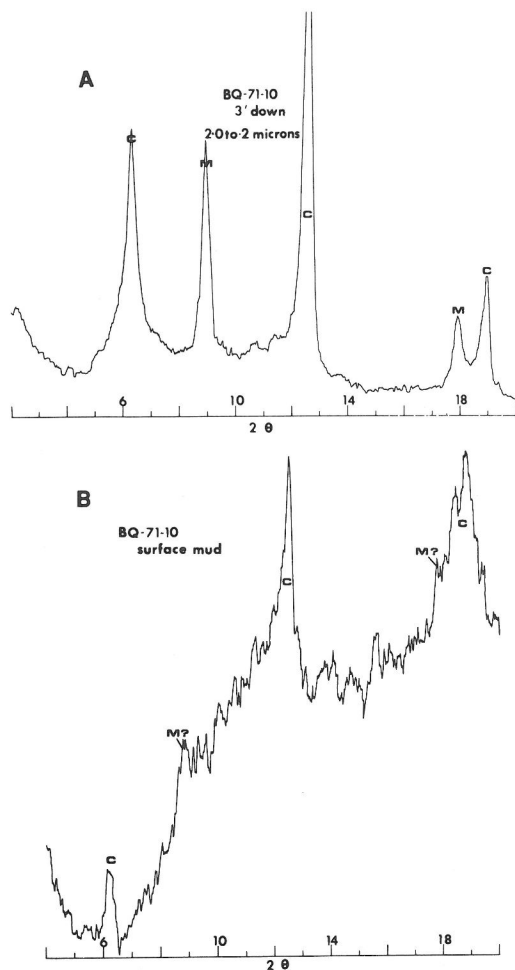


FIG. 3. X-ray diffraction patterns of fine fraction of muds at station BQ-10. Fig. 3A low 2θ region of the fine fraction of muds from 0.9 m depth. These muds are isolated from the aquifer and lake waters. Fig. 3B, low 2θ region of fine fraction of surface muds (ooze) contacted by spring and early summer brines. C = 14 Å chlorite; M = 10 Å mica.

The Basque Lake Basin is very small and the recharge, and probably the entire hydrological regime, is local (TOH, 1963). Brines are present in the lake throughout the summer period and as emphasized by GOUDGE (1924), the 'conical springs' of the lake flow rapidly when exposed at depth. Apparently the springs are hydrologically connected to a reservoir but again the only likely one is the sandy reservoir. If so, the volcanic ash aquifer, and probably sandy units near the base of the sedimentary pile, provide the hydrological connection between the springs and the reservoir (Fig. 2B). The waters of the aquifer and lake are the $Mg-Na-SO_4$

type (Table 1), indicating a common geochemical and hydrological origin. Furthermore, the waters of the aquifer are most dilute closest to the perimeter of the basin, suggesting that they are replenished from the perimeter (*i.e.*, connected to the sandy reservoir). Detailed hydrological studies are required to confirm the deductions.

Salinity of the waters in the aquifer increases towards the lake (Table 1, Fig. 1B). Impermeable muds overlying the aquifer inhibit evaporative concentration but evapotranspiration occurs, as is evident by the presence of luxuriant grasses on the valley floor during even the driest parts of the summer. The high salinities may result, in part, by diffusion of dissolved salts from the lake brine into the aquifer.

Unaltered glass of the ash horizon has refractive indices ranging from 1.508 to 1.512, indicating Mazama glass (Crater Lake), which has been recognized at other localities close to Basque Valley (POWERS and WILCOX, 1964). The glass is approximately 6000 years old. The thickening of the ash horizon towards the lake indicates that it has been transported somewhat after deposition. Ash deposited around the perimeter of the basin may have been transported to the basin floor, resulting in comparatively thick ash in the central, lowest portions of the basin floor and no ash on flanks.

GOUDGE (1924) collected a brine sample from Basque No. 2 Lake (Table 1, Fig. 1B, BQ-24) and its composition is almost identical to one collected in 1970 (Table 1, BQ-3). The similarity suggests that the hydrological and chemical systems have been stable over at least the last 50 years.

AUTHIGENIC SALTS OF THE BASIN

Authigenic Ca- and Mg-carbonates are found within the ash aquifer and in muds immediately adjacent to the aquifer. The distribution of carbonates in hole BQ-13 is typical. Mud at 45 cm contain little authigenic carbonates (Fig. 4A), but sediments within 7 cm of the aquifer (63–70 cm below floor) contain abundant carbonates (Fig. 4B). The ash (70–75 cm depth) contains carbonate (Fig. 4C) but less than the immediately adjacent muds. Similar relations exist below the ash horizon. The carbonates are abundant in the fine grained 2.0 to 0.2 micron fraction of the muds. The observations support an authigenic origin, where the carbonates have formed from the waters of the aquifer as a result of concentration of the aquifer waters in the subsurface.

The $MgCO_3$ content of calcite and protodolomite

Table 1. Basque Lake #2 Basin water compositions (mmoles/l)*

Species	BQ-7	BQ-6	BQ-5	BQ-4	BQ-3	BQ-24	SP-2
HCO ₃	11.60	15.47	15.88	21.96	46.16	48.50	2.26
SO ₄	146.78	142.62	185.30	1249.20	2529.63	2424.60	8.12
Cl	2.71	1.89	3.47	15.15	99.30	155.80	0.22
F	0.38	0.33	0.41	0.84	0.89	ND	0.05
Ca	8.86	9.08	9.76	43.17	21.88	ND	3.50
Mg	117.63	115.17	150.13	970.67	1711.10	1749.00	2.68
Na	51.33	51.33	66.12	452.40	1533.45	1347.80	6.09
K	2.40	2.56	3.07	21.04	127.08	163.70	0.38
Sr	0.09	0.09	0.23	0.32	0.46	ND	—
Al	3.40	3.70	4.80	35.00	59.00	ND	—
SiO ₂	0.15	0.20	0.18	0.07	—	ND	0.03
pH**	7.25	6.98	7.04	6.86	8.10	ND	7.60
T (C)	11.50	11.50	11.00	17.00	35.00	ND	12.00
BAL (%)	-0.441	-0.119	-0.238	-1.364	-1.502	-0.871	0.32

ND = not determined; — = not detected.

* Values in M/l $\times 10^3$ except for Al which is in mg·l.

** pH was measured in the field at the temperature indicated. Chemical analyses performed by S. Rettig, under the supervision of B. F. Jones, U.S. Geological Survey Laboratories, Reston, Va.

were determined using the data of GOLDSMITH *et al.* (1961). An error of ± 3 mole percent is assigned to all MgCO₃ contents due to uncertainty in the data. Calcite and protodolomite peaks are separated by slightly more than $1^\circ 2\theta$ and where one peak is greatly dominated by the other peak, there is the possibility of error in measuring the MgCO₃ content of the less abundant phase. Errors of this type, however, are insignificant. Even for the MgCO₃ content of calcite in BQ-9 (Fig. 5F) the corrections remain within the ± 3 percent assigned error.

Calcite

X-ray diffraction patterns of muds adjacent the aquifer at BQ-8 (Fig. 2) indicates that calcite is a minor constituent compared with quartz (Fig. 5A). It is a major constituent of the muds adjacent the aquifer at BQ-12 (Fig. 5B) and at BQ-7 (Fig. 5C). Calcite is less abundant in muds adjacent the aquifer of BQ-10 (Fig. 5D), is diminished at BQ-9 (Fig. 5E) and is absent from the ooze of the lake at BQ-2 (Fig. 4F). There is systematic increase of calcite from BQ-8 to BQ-7 but it decreases in abundance in samples closer to the lake and is absent from the oozes of the lake.

The MgCO₃ content and relative abundance of calcite is given in Table 2. Calcite in BQ-8 contains 8 mole percent MgCO₃, which increases to 10 mole percent in BQ-7. The MgCO₃ increases still further to 29 percent in samples near the lake (BQ-10 and BQ-9).

Protodolomite

Protodolomite is absent from BQ-8 and BQ-12 but is present in moderate quantity at BQ-7 (Fig. 2, Fig. 4C). Its relative abundance increases towards the lake (Fig. 4D) compared with quartz, feldspar and calcite (Fig. 4D, 4E, and 4F) and is a major constituent of the muds fringing and within the lake (Fig. 4E and 4F). Like calcite, protodolomite is most abundant in the fine fraction of the muds. Super-

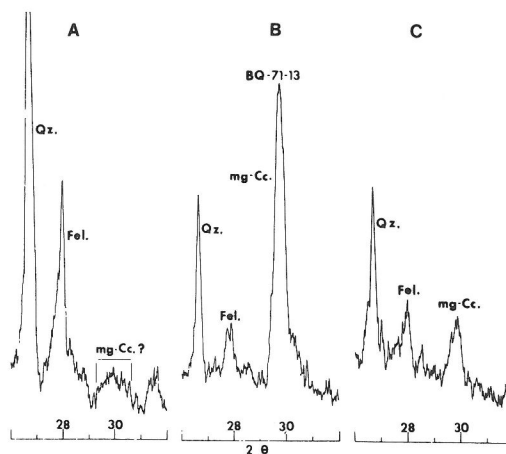


FIG. 4. X-ray diffraction patterns of muds from BQ-13. Fig. 4A is an X-ray diffraction pattern of muds 30 cm above the volcanic ash aquifer. Fig. 4B a pattern of mud 5-10 cm above the aquifer and Fig. 4C is a pattern of the volcanic ash (the aquifer). Qz = quartz; Fel = feldspar; Mg-Cc = Mg-calcite.

structure peaks have not been observed, suggesting that the protodolomite is essentially disordered and may best be assigned to the $R\bar{3}_c$ space group (calcite structure) rather than the $R\bar{3}$ space group of ordered dolomite.

Protodolomite changes composition systematically within the basin (Table 2). At BQ-7 its composition is 32 ± 3 mole percent $MgCO_3$ but the percentage increases to 43 ± 3 mole percent at BQ-10, BQ-9 and BQ-2.

Magnesite and gypsum

Magnesite and gypsum are found in the surface muds of BQ-10 (Fig. 5). The two minerals are discussed together because there is uncertainty as to which has formed first.

Magnesite has been found only in the fine fraction of the muds ($>2 \mu$ fraction) and nowhere is it abundant. It is not observed on X-ray diffraction patterns of the bulk sediment (Fig. 4 represent patterns of bulk sediment), probably because of its low abundance and is found only in fine grained separates. The magnesite lattice parameters are slightly greater than those of stoichiometric, coarse grained and well crystallized magnesite.

Gypsum is first observed at BQ-10 where it is present in minor amounts. It is, however, dispersed throughout all muds contacted by lake brine. In these oozes, gypsum crystals range from fine to coarse grained euhedral to subhedral. It is the first sulphate to form from the lake waters as they are evaporated during the early summer months.

Epsomite and bloedite

Epsomite ($MgSO_4 \cdot 7H_2O$) and bloedite ($Na_2Mg(SO_4)_2 \cdot 2H_2O$) form from the concentrated lake brines during the mid and late summer. They precipitate as individual, fine to coarse grained crystals and aggregates, forming caps and crusts over the brine.

AUTHIGENIC MINERAL ZONES OF THE BASIN

Mineral zones of the valley floor are defined by the assemblage of authigenic carbonates found in muds adjacent to the aquifer. The calcite zone (*Cc zone*) is closest to the perimeter of the basin (farthest removed from the lake). BQ-8 and BQ-13 are within this zone (Fig. 2). BQ-12 contains protodolomite as well as calcite. This assemblage represents the second zone, (*Cc-Pr zone*). The boundary separating the two zones is between BQ-13 and BQ-12 (Fig.

2). The authigenic sulphates of the surface muds within the lake are used to define additional zones. A unique mineral assemblage exists between the high-water and low-water marks of the lake. Magnesite and gypsum and protodolomite are found in the zone (Fig. 6) but gypsum is used to define the zone and is referred to subsequently as the gypsum zone (*Gyp zone*). The final zone is the area within the low-water mark of the lake. Authigenic Mg- and Na-sulphates are characteristic of this zone and it is referred to subsequently as the epsomite zone (*Ep zone*). Gypsum is ubiquitous in the zone and magnesite and protodolomite are common.

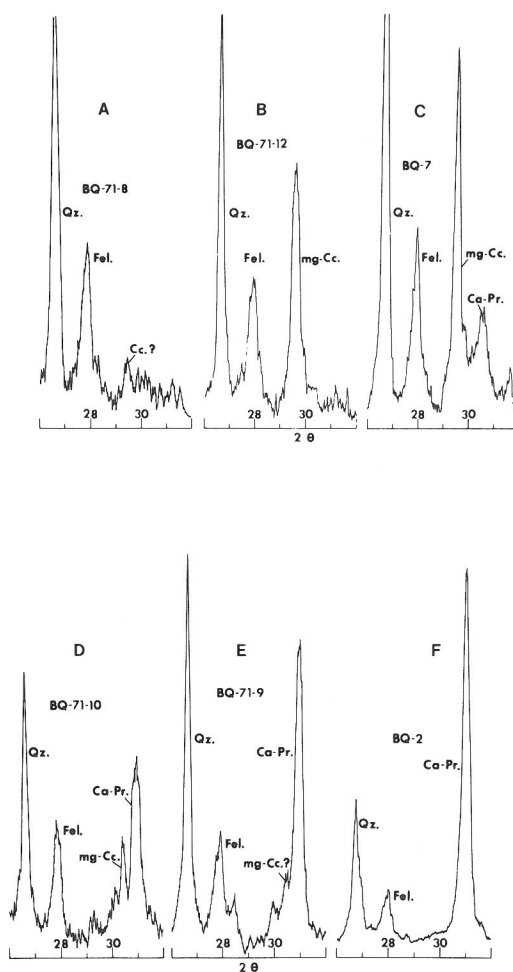


FIG. 5. X-ray diffraction patterns of muds from within the Basque Basin. The patterns illustrate the changing proportions and compositions of authigenic carbonates relative to proximity of the lake. The sites are arranged with Fig. 4A the sample farthest from the lake and Fig. 4F a sample of lake mud (see Fig. 2 for specific locations). Ca-Pr = Ca-protodolomite, other abbreviations as in Fig. 4.

Table 2. XRD data of carbonates from Basque Lake #2 Basin

Phase		BQ-8	BQ-13	BQ-7	BQ-10	BQ-9	BQ-2
Mg-Cc	2 θ (104):	29.65	29.78	29.75	30.4	30.45	—
	% MgCO ₃ :	8	11	10	29	30	
	Amount:	DET.	MAJOR	MAJOR	MOD.	DET.	
	2 θ (104):	—	30.55	30.5	30.9	30.9	30.9
	% MgCO ₃ :		33	32	43	43	43
Ca-Prot	Amount:		MINOR	MOD.	MAJOR	MAJOR	MAJOR

DET. = Detectable; — = Not detected; MOD. = Moderate.

COMPOSITIONS OF THE WATERS

Compositions of the waters of the basin and one inflow water (SP-2) from Spotted Lake Basin are included in Table 1 and plotted on Fig. 7. The most dilute waters from the Basque Basin were collected from the volcanic ash aquifer at BQ-6 and BQ-7, near the head of the valley (Fig. 2) but the waters become progressively more saline towards the lake. No sulphate salts have been found within the muds adjacent to the aquifer and no chloride salts have been found anywhere in the basin. Chloride ion is used as a 'tracer' to calculate the concentration factor for each water relative to BQ-6. The logarithm of the concentration factor (abscissa) and the logarithm of the concentration of the aqueous species (ordinate) are plotted on Fig. 7. Concentration-dilution trends are calculated for each species. The trends are straight, of unit slope, and emanate from BQ-6 water. If species for other waters plot on the concentration-dilution trend, then their concentrations can be derived by concentrating (or diluting) BQ-6. Species extracted from solution during concentration plot below the concentration-dilution trend and species added to solution during concentration plot above it.

General compositional trends

BQ-6 water must be concentrated almost 100-fold (concentration factor) to obtain the Cl content of the lake brines. Waters within the aquifer are concentrated 10-fold through evapotranspiration by the valley grasses and the second 10-fold concentration occurs in the lake through solar evaporation.

Anions

SO₄ (Fig. 7A, solid squares) follows the concentrative trend from BQ-6 to BQ-4 but the brines BQ-3 and BQ-24, plot below the trend, indicating that SO₄ has been extracted from the brines. Sulphate of SP-2 plots close to the concentration trend for the Basque Basin, indicating that SO₄/Cl of the very dilute input waters to the Spotted and Basque Lake Basins are similar. HCO₃ for samples of

the Basque Basin plot below the concentration trend, hence it is lost from the more concentrated waters of both the aquifer and lake of the Basque Basin. Sample SP-2 plots close to the concentration trend, indicating that HCO₃/Cl of SP-2 and BQ-6 are similar. Fluoride is lost from the waters of the aquifer and lake. Although fluorite has not been found in the basin it would precipitate in small quantities and may have been present but remained undetected. F/Cl of sample SP-2 is similar to that of BQ-6.

Cations

Mg of samples BQ-6 to BQ-4 plots close to the concentration trend, thus there is little Mg lost from the aquifer waters during concentration. Carbonates, however, are found in and adjacent to the aquifer. Apparently, and although Mg is removed to form of Mg-calcite and proto-

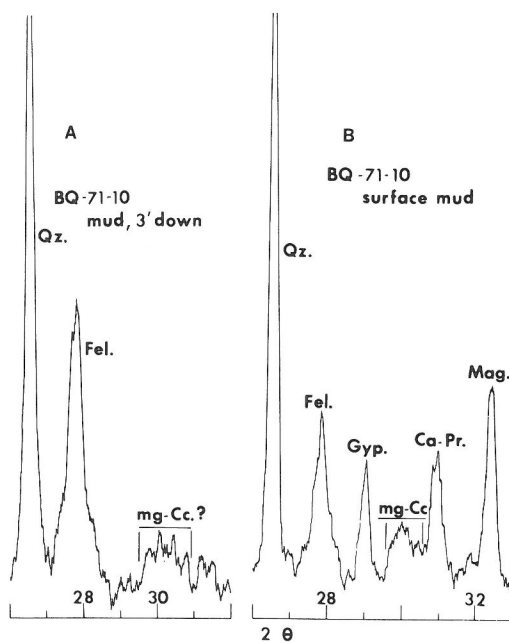


FIG. 6. X-ray diffraction patterns of muds at BQ-10. Fig. 6A is a sample of muds from 0.9 m depth (divorced from aquifer and lake waters). Fig. 6B is a pattern of surface mud. Gyp = gypsum; Mag = magnesite, other abbreviations as in Fig. 4 and Fig. 5.

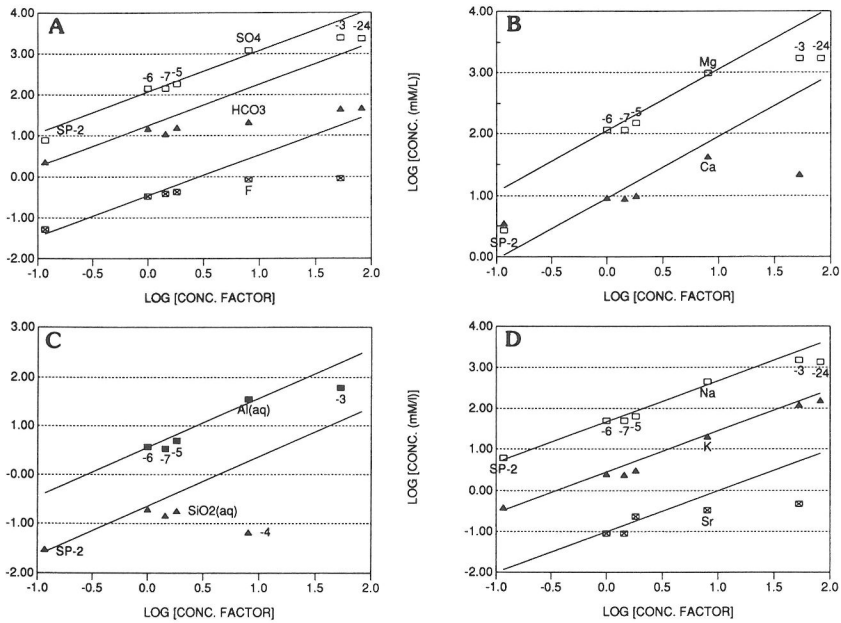


FIG. 7. Compositional trends for the Basque and Spotted Lake Basin waters. Concentrations of individual species are plotted against the concentration factor for each water (abscissa). Straight lines represent concentration-dilution curves for a water compositionally similar to BQ-6.

dolomite, the amount extracted is insignificant compared with the quantity in solution. Mg data for the lake brines (BQ-3 and BQ-24) plot well below the concentration trend, hence large amounts of Mg are removed during concentration of the brines. Epsomite and bloedite are precipitated from the brines. Mg of SP-2 plots well below the concentration curve, indicating that Mg/Cl is much lower than Mg/Cl of the dilute input waters to the Basque Basin. The calcium trend of the Basque Basin waters plots below the calculated concentration trend; Ca is removed from the waters of both aquifer and lake. SP-2 plots above the BQ-6 concentration trend indicating that Ca/Cl is greater than in the dilute Basque Basin input waters. Sodium of the aquifer waters (BQ-6 to BQ-4) and SP-2 plot on the BQ-6 concentration trend, indicating that Na/Cl are all similar. The lake brines, however, plot below the concentration trend, hence Na has been extracted from the brines during concentration. Strontium in BQ-6, BQ-7 and BQ-5 plot close to the concentration curve but BQ-4 plots below the curve and BQ-3 is still more depleted. Sr-bearing phases have not been identified but minerals such as strontianite or celestite may form; alternatively Sr may be taken into the Ca-Mg-carbonates in quantities sufficient to affect Sr contents of the basin waters.

Potassium of all waters from the Basque Basin and of SP-2 plot close to the concentration curve, thus all waters have similar K/Cl ratios. Apparently little K is removed from either the aquifer or lake waters. Aqueous aluminium of the aquifer waters plots close to the concentration trend but the Al(aq) of the brine (BQ-3) plots well below the trend. Apparently little Al is lost from solution within the aquifer but appreciable quantities are lost from the brines. Ooze contacted by brines displays much different XRD patterns from other muds of the basin (discussed subse-

quently). Al may be taken up by the oozes of the lake. Aqueous silica of the aquifer waters plots well below the calculated trend and its concentration is below detectability in the lake brines. Apparently it is extracted from the aquifer and lake waters during concentration.

Mass balances for waters of the aquifer

Cl and SO_4 are conservative in waters from the aquifers, hence either species may be used to calculate concentration factors (Table 3, bottom two rows). The Cl content of BQ-6 is low compared with SO_4 (Table 1), hence small errors in analyses or minor but real variations in Cl contents introduce relatively large errors in calculated concentration factors and mass balances. The more abundant SO_4 is used to calculate concentration factors. Gains and losses (mass balances) required to derive BQ-7, BQ-5 and BQ-4 from BQ-6 are listed in Table 3. A negative value indicates the species must be extracted from BQ-6 during concentration; a positive value indicates addition.

HCO_3 is lost during concentration of BQ-6 to BQ-7. The small negative and positive values for the other species reflect errors associated either with the analysis or with natural variations in the concentrations of the species. Mass balances between BQ-6 and BQ-7 are too small to be interpreted with confidence.

Table 3. SO₄-Cl derived mass balances relative to BQ-6

Species	BQ-7	BQ-6	BQ-5	BQ-4	BQ-3	BQ-24	SP-2
HCO ₃	-4.3	0.0	-4.2	-113.5	-766.6	-1226.8	0.5
SO ₄	-CF-	-CF-	-CF-	-CF-	-4963.6	-9332.1	-8.5
Cl	0.8	0.0	1.0	-1.4	-CF-	-CF-	-CF-
F	0.0	0.0	-0.0	-2.1	-16.4	-27.2	0.0
Ca	-0.5	0.0	-2.0	-36.4	-455.2	-748.5	2.4
Mg	-0.9	0.0	0.5	-38.1	-4339.9	-7744.9	-10.7
Na	-1.5	0.0	-0.6	2.8	-1163.4	-2883.5	0.1
K	-0.2	0.0	-0.3	-1.4	-7.4	-47.3	0.1
Sr	-0.0	0.0	0.1	-0.5	-4.3	-7.4	-0.0
Al	-0.4	0.0	-0.0	2.6	-135.4	-305.0	-0.4
SiO ₂	-0.1	0.0	-0.1	-1.7	-10.5	-16.5	0.0
pH	7.25	6.98	7.04	6.86	8.10	ND	8.10
BAL (%)*	28.143	0.0	14.34	26.870	0.554	0.07	-0.62
CF (SO ₄)**	1.029	1.00	1.299	8.75	17.737	17.00	0.06
CF (Cl)†	1.434	1.00	1.836	8.016	52.540	82.434	0.12

-CF- = Species used to calculate Concentration Factor of the sample.

ND = Not Determined.

* Charge balance for each water.

** Value of conc. factor based on sulphate.

† Value of conc. factor based on chloride.

BQ-5 is concentrated 1.3 times relative to BQ-6, and to derive BQ-5, from BQ-6, Ca and HCO₃ has to be removed in the ratio of approximately 1:2. The mass balances are consistent with the reaction:



Gains or losses of the other major constituents are insignificant.

BQ-6 must be concentrated 8.8 times to achieve SO₄ levels of BQ-4. Large quantities of HCO₃, Ca and Mg are extracted from solution (Table 3) and HCO₃/(Ca + Mg) of the material removed is 3:2. A more accurate mass balance can be constructed if waters BQ-6 and BQ-4 are first corrected for their charge imbalance (Table 1). Sulphate and Mg are the most abundant species by far and most likely small analytical errors in SO₄ and/or Mg account for much of the imbalance. The charge imbalance of BQ-4 can be corrected by increasing Mg of Table 1 by 1.8 percent, or by decreasing SO₄ by 1.4 percent. Correction first to SO₄, and next to Mg, indicates that HCO₃ and Ca + Mg are extracted in the ratio 1.84:1 and 1.94:1. Fluoride is lost during concentration of BQ-6 to BQ-4 and probably as fluorite. Correction to Ca for fluorite precipitation increases HCO₃/(Ca + Mg) to 1.87:1 and 1.98:1. The ratios are close to the that required by reaction (1), which is 2:1. The corrected data also demonstrate that more CaCO₃ is removed from solution than MgCO₃ during concentration of BQ-6 to BQ-4.

Mass balances for lake brines

Cl is used to calculate concentration factors for the lake brines. BQ-6 is concentrated 52.5 and 82.4 times to achieve Cl contents of BQ-3 and BQ-24. SO₄, Mg and Na are extracted from solution during concentration (Table 3) as gypsum, epsomite and bloedite (Table 4) and SO₄ is reduced. The amount of salts precipitated during evolution of successively more concentrated waters, normalized to unit concentration factor, is shown in Table 4. Carbonates form in large quantity both between BQ-5 and BQ-4, and from the lake brines (Table 4). The largest amounts of gypsum and epsomite (per unit of concentration) are precipitated during concentration of BQ-4 water to BQ-3. The amount of epsomite, however, is subject to error in that the amount the calculation does not include a correction for sulphate reduction. Bloedite is produced in greatest amount during the most extreme stage of concentration (BQ-3 to BQ-24). The mass balance relations correspond closely with the authigenic mineral zones.

There is loss of Al, Si and smaller amounts of K during concentration of the lake brines. These elements commonly are found in the silicate minerals and they may be removed from solution to form authigenic Al-bearing silicate minerals in the oozes. Although individual authigenic silicate minerals have not been identified from the lake muds, the XRD patterns of the clay minerals (Fig. 3) dem-

Table 4. Grams of salts produced¹ from solution

Salts	BQ-6	6-7/CF ²	6-5/CF	5-4/CF	4-3/CF	3-24/CF
BLOEDITE ³	0.0	0.0	0.0	0.0	109.2	337.2
CARBONATE ⁴	2.2	0.0	1.6	6.3	7.5	7.6
GYPSUM ⁵	0.0	0.0	0.0	0.0	36.1	18.1
EPSOMITE ⁶	0.0	0.0	0.0	0.0	608.7	291.8
EPSOMITE ⁷	0.0	0.0	0.0	0.0	596.7	255.3

¹ Amounts normalized to unit concentration factor.

² Loss/gain from BQ-6 to BQ-7 divided by CF for BQ-7 (calc. using BQ-6 as parent).

³ Calculated assuming that Na is removed as Bloedite.

⁴ 1/2 of HCO₃ removed forms carbonate (rxn 1).

⁵ Calculated: GYPSUM = Ca(T) - 0.5 * CARBONATE.

⁶ Calculated: EPSOMITE = SO₄(T) - 2 * BLOEDITE - GYPSUM.

⁷ Calculated: EPSOMITE = Mg(T) - BLEODITE - 0.5 CARBONATE. Comparison with 6 provides a check on how much of sulphate is reduced in the lake muds.

onstrate a substantial change to the properties of the bulk clays.

DISTRIBUTION OF Mg AND Ca BETWEEN SOLUTION AND CALCITE

MUCCI *et al.* (1985) report the compositions of Mg-calcite overgrowths on pure calcite seeds and of the associated solutions. They demonstrate that the overgrowths remain in exchange equilibrium with solution even though the solutions are slightly to greatly supersaturated with respect to the original calcite seed crystals. The findings support earlier observations (GARRELS and WOLLAST, 1978). There remains, however, well justified concern that

kinetic aspects strongly influence or even control the amount of Mg incorporated into calcite from solutions (BERNER, 1975, 1978; THORSTENSON and PLUMMER, 1977, 1978). The Basque solutions and calcite compositions can be used to test if exchange equilibrium is maintained between solution and authigenic Mg-calcite in natural settings.

The solutions used by MUCCI *et al.* (1985, Table 2) were subjected to a thermodynamic evaluation using the 'WATEQ' program (TRUESDELL and JONES, 1974). The activity proportion, [Mg]/([Mg] + [Ca]), was calculated (square brackets denote activities) for each water. The molar proportion of Mg in calcite, Mg/(Mg + Ca), was also calculated with all results plotted on Fig. 8. Activity or molar proportions of the solids can be used here, as discussed subsequently. Tie-lines connect the activity proportions of each experimental solution to the molar proportion in the respective Mg-calcite. The tie-lines represent exchange equilibrium between the two phases.

The same thermodynamic treatment has been performed on waters from BQ-7 and BQ-4 (Table 1) to obtain the activity proportions [Mg]/([Mg] + [Ca]), and the molar proportions of Mg in calcite associated with these waters also have been calculated and plotted on Fig. 8. Calcite of BQ-7 contains 10 ± 3 mole percent MgCO₃ (Table 2). Sample localities BQ-4 and BQ-10 are within 50 cm of one another. Calcite from BQ-10 contains 29 ± 3 mole percent MgCO₃ and the solution from BQ-4 is representative of the waters from this part of the aquifer. The tie-lines connecting BQ-7 and BQ-4 waters to their respective calcite compositions are shown on Fig. 8 (thick lines). The data of MUCCI *et al.* (1985) and Basque Basin data are indistinguishable. The BQ-4/BQ-10 tie-line plots at the extreme of the

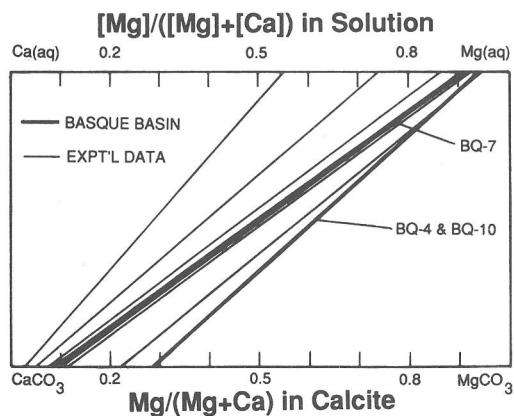


FIG. 8. Tie-line diagram illustrating the Mg-Ca distribution between solution and calcite. Upper axis represents Mg molar proportion in solution whereas the lower axis represents Mg molar proportion in calcite. Thin tie-lines are constructed from experimental data (MUCCI *et al.*, 1985) and the thick tie-lines are constructed using field data from Basque Valley.

MUCCI *et al.* (1985) data. Although the slope is somewhat steeper than the closest tie-line of MUCCI *et al.* (1985), the BQ-4/BQ-10 and experimental tie-lines are within analytical error (± 3 mole percent for each experiment). There is strikingly good agreement between the experimental and Basque Lake Basin data. The exchange equilibrium hypothesis is used to model the evolution of the Basque Basin waters and carbonates.

Carbonate minerals produced in the Basque Basin and in the experiments of MUCCI *et al.* (1985) contain CaCO_3 and MgCO_3 as the only essential components. The solid solution is binary for both environments, thus activity coefficients are the same for the two components in Mg-calcites with the identical composition in the two settings. As a result, the conclusions drawn from this comparative study are valid whether mole proportions or activity proportions are used. Only where the actual chemical potentials of components are required (*i.e.*, for arguments based on saturation indices) are activities needed.

There is an important difference between the experimental results and results from Basque Basin; protodolomite is found in the basin. It may not have formed in the laboratory for lack of an appropriate seed on which to grow. Alternatively, supersaturation levels required to form protodolomite were not achieved in the experiments. MUCCI *et al.* (1985) provide evidence that exchange equilibrium exists between dolomite and solution. It is likely, therefore, that there is exchange equilibrium between protodolomite and solution, particularly in the Basque Basin where the protodolomite is structurally indistinguishable from very high Mg-calcite.

FORMATION OF SALT ZONES AND EVOLUTION OF SOLUTIONS

The consistent relationship between mineralogic zones and water compositions may be genetic, and a thermodynamic model is constructed to test the possibility. Development of the model is found in the appendix and the results are summarized in Fig. 9. It portrays equilibrium between solutions and the salts calcite, protodolomite, magnesite, gypsum and epsomite. The abscissa is $\text{Mg}/(\text{Mg} + \text{Ca})$ (solution or salts) and the ordinate is $\text{SO}_4/(\text{SO}_4 + \text{HCO}_3)$ in solution or salts. The mineral compositions are illustrated by squares and Mg-calcite and Ca-protodolomite solid solutions by bars (Fig. 9). The epsomite stability field has been expanded for clarity but geometric relations are preserved. Field boundaries delimit compositions of solutions

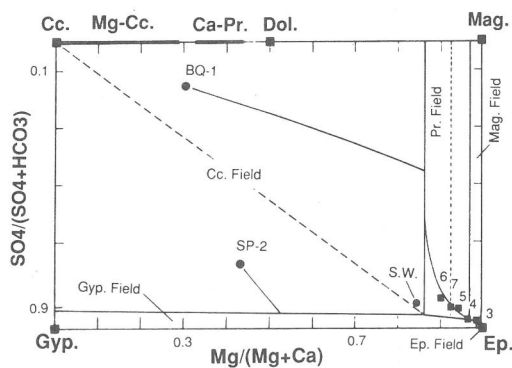


FIG. 9. Stability diagram for the system $\text{CaCO}_3\text{-MgCO}_3\text{-CaSO}_4\text{-MgSO}_4$. The ordinate and abscissa represent respectively, $\text{SO}_4\text{-HCO}_3$ and Mg-Ca molar proportions. The thick lines delimit the stability field of each salt (*e.g.* Cc field). The dotted line separates two great groups of waters (see text). The waters of Table 1 are plotted on the diagram (BQ- prefix omitted) as is seawater (S.W.) and the hypothetical water BQ-1. Thin lines emanating from BQ-1, SP-2 and S.W. illustrate their evolution during concentration. The compositions of calcite, Mg-calcite, protodolomite, magnesite, gypsum and epsomite are plotted (squares or solid bars on boundaries).

equilibrated with each of the labelled salts. The boundaries are of the eutectic (calcite-gypsum boundary) and peritectic (calcite-protodolomite) types. A solution that plots within the stability field of a salt, when concentrated, becomes saturated in that salt first, and by the equilibrium model, it is the first to precipitate. The solution evolves directly away from the composition of the precipitated salt, as required by mass balances. Similar mass balance arguments are applicable at boundaries and at triple points.

Predictions of the equilibrium model

The hypothetical water BQ-1 (Fig. 9) plots within the calcite stability field, hence during concentration of the water calcite is predicted to precipitate first. As a result, the solution composition evolves away from calcite composition (solid curve emanating from BQ-1). Mg/Ca increases in the evolved solution (Fig. 9) as a result of calcite precipitation. Equilibrium thermodynamic constraints require the composition of precipitated calcite to change towards a higher Mg content in response to changing water composition. The evolutionary path of BQ-1 therefore is curved. As concentration of BQ-1 continues, $\text{Mg}/(\text{Mg} + \text{Ca})$ increases in solution until the calcite-protodolomite boundary is intersected. Both calcite and protodolomite compositions plot

to the left of the boundary, thus it is a peritectic, or reaction boundary. Two extreme situations arise at the boundary. One, referred to as the closed system, allows for all calcite previously precipitated to react with the evolved solution, and the other, the open system, requires all precipitated salt to be isolated from solution as it forms, and to remain isolated subsequently. Natural settings fall between these extremes.

After BQ-1 encounters the peritectic curve, continued concentration results in the conversion of calcite to protodolomite. During conversion, the solution composition evolves down the peritectic curve towards the calcite-protodolomite-gypsum peritectic triple point. The mechanism of conversion is of no consequence to the equilibrium model. If conversion is complete before the solution composition reaches the triple point, an additional degree of freedom is gained and the solution leaves the peritectic curve and migrates through the protodolomite field. The path traced by the evolving solution is determined by the composition of the protodolomite formed. If the solution encounters the triple point before all calcite is consumed, the solution remains at the peritectic point until conversion is complete. Thereafter, the solution evolves along the protodolomite-gypsum eutectic curve with the two phases co-precipitating. At the protodolomite-gypsum-magnesite peritectic point, all protodolomite previously formed reacts with solution to produce gypsum + magnesite. Once protodolomite is consumed, the solution migrates down the gypsum-magnesite eutectic curve to the gypsum-magnesite-epsomite eutectic point, where epsomite co-precipitates with gypsum and magnesite.

Interpretation of the peritectic reaction is not as simple as presented above. The peritectic curve (Fig. 9) represents reaction between a calcite and protodolomite of fixed composition. Since both carbonates display extensive solid solution and there is exchange equilibrium amongst the phases, there exist many peritectic curves (in fact a continuum), one for each combination of calcite-protodolomite compositions. A dotted peritectic curve is plotted within the protodolomite stability field (Fig. 9) as an example; it represents the peritectic boundary for the calcite and protodolomite composition of BQ-7 (Table 2). The path of a solution cannot be calculated without knowing how carbonate compositions change as the solution evolves. Exchange constants for calcite and solution are known, but there are no data for Ca-protodolomite solid solution. Data from MUCCI *et al.* (1985) are helpful in that exchange equilibrium between dolomite over-

growths and solution is shown to be maintained, but exchange constants are not yet available. As a result, the path of the solution while on the peritectic curve is constrained but cannot be calculated accurately. Some constraints are now discussed.

Mg-calcites of different compositions are distributed (systematically) throughout the basin, the low Mg-calcites having formed from the least evolved waters in the upper reaches of the basin, and the high Mg-calcites having formed from more evolved waters. The calcite-protodolomite peritectic boundaries applicable to each sample will be dependent on the Mg-Cc and Ca-Pr compositions. From exchange equilibrium principles, the peritectic boundary applicable to the least Mg-rich carbonates is associated with solutions of the lowest Mg/(Mg + Ca) values, which are the less evolved solutions near the flanks of the valley. The peritectic curve applicable to Mg-rich carbonates is associated with solutions of high Mg/(Mg + Ca) values which are the more evolved solutions found close to the lake. Peritectic curves are, therefore, spatially separated in the Basque Basin. During concentration, any solution plotting on a peritectic curve not only evolves down the curve, but shifts to new peritectic curves representative of new carbonate assemblages encountered as the solution migrates through the aquifer. As a result of migration, the solution encounters carbonate assemblages ever more enriched in Mg, hence the solution must shift to peritectic curves plotting at successively high Mg/(Mg + Ca) values on Fig. 9; thus, the solution increases in Mg/(Mg + Ca) even as it evolves down successive peritectic curves. The curved solution path (Fig. 9) passing through the Basque samples represents such a path. Eventually Mg-calcite is consumed, the peritectic reaction ceases and protodolomite alone forms as the solution composition evolves through the protodolomite stability field to the protodolomite-gypsum or protodolomite-magnesite boundary.

Water compositions

The BQ-1 water (hypothetical) is predicted to evolve towards high $SO_4/(SO_4 + HCO_3)$ and Mg/(Mg + Ca) values. As is apparent from the data of Table 1, these predictions are correct. The exceedingly dilute waters of the aquifer associated with spring runoff have not been collected, and additional study is required in this regard. A critical test of the equilibrium model will be to collect the dilute aquifer solutions and monitor compositional changes during the spring and early summer months to see if they evolve as predicted.

Authigenic salt zones

The equilibrium model offers an explanation for the major aspects of the authigenic salt zones. The predicted authigenic salt sequence obtained during the concentration of BQ-1 are, for the open and closed systems:

<u>Closed System</u>		<u>Open System</u>
Gyp + Mag + Ep	Last to precipitate	Gyp + Mag + Ep
Gyp + Mag Ca-Pr + Gyp + Mag		Gyp + Mag Gyp
Ca-Pr + Gyp Mg-Cc + Ca-Pr		Mag Ca-Pr
Mg-Cc	First to precipitate	Mg-Cc

The sequences are similar to the authigenic mineral zones and there remains little doubt that the thermodynamic model provides a reasonable explanation for the evolution of the Basque Basin waters and salt zones. Complexities exist, however, because the zones develop in time and space. Ambiguities result where water compositions are related to these variables but an attempt is made to relate the three aspects. Dilute runoff accumulates in the aquifer during early spring. Waters are concentrated in the aquifer during the summer by evapotranspiration and the waters follow evolutionary paths similar to BQ-1 (Fig. 9). The waters of the aquifer are concentrated as they migrate towards the lake and the Mg content of progressively more concentrated waters increases due to the precipitation of calcite, hence calcites of greatest Mg content are found closest to the lake. Protodolomite forms after calcite, from still more concentrated waters, hence is formed in a zone close to the lake.

The antipathetic relationship between calcite and protodolomite contents of the muds result from the peritectic reaction among solution, calcite and protodolomite, but is complicated by the yearly hydrological cycle. During late summer, waters in the aquifer are more concentrated than spring runoff waters. Low Mg-calcite precipitated early during the summer may be contacted by solutions of the late summer. If Mg/(Mg + Ca) is sufficiently high, early formed calcite reacts with the evolved late summer solution to form protodolomite and to yield an antipathetic relationship between the calcite and protodolomite contents of the muds.

The late summer brines of the lake are restricted to local 'pools' (GOUDGE, 1924). Salts precipitated

in these pools during the spring and early summer are available to react with the evolved brines of late summer, hence closed system constraints prevail within the brine pools and peritectic reactions should occur. Salts precipitated outside of the local 'pools' (e.g., mud flats) are not contacted by the late summer brines, thus constraints of the open system prevail in the mud flats, and peritectic reactions should be much less important. As a result, the assemblage gypsum + magnesite + epsomite is predicted within the pools but gypsum + protodolomite (\pm calcite) should be more common on the mud flats. These predictions again explain the major features of the salt zones of the lake area. Epsomite and gypsum (+ bloedite which is outside the compositional space considered here) are the dominant authigenic salts of the 'pools' whereas gypsum and protodolomite are the most abundant salts in the mud flats.

REACTIONS BETWEEN SILICATE MINERALS AND SOLUTIONS

Muds of the basin are composed of feldspars, quartz and phyllosilicates, primarily illite and chlorite (Fig. 3A). The peaks are well defined with but small shoulders developed on the low 2θ side of the 10 Å mica and 14 Å chlorite peaks. The ooze of the lake muds present a sharp contrast; the 10 Å mica peak is difficult to detect and the 14 Å ($6^\circ 2\theta$) chlorite peak is greatly diminished and ragged. There is an exceptionally high background, in the region between 8° and $30^\circ 2\theta$ (Fig. 3B), perhaps resulting from the presence of X-ray amorphous Si- and Al-bearing solids. The solutions indicates reaction with silicates. $\text{SiO}_2(\text{aq})$ is comparatively abundant in the most dilute samples (Table 1), is less abundant in the more concentrated aquifer waters and is not detectable in the brine (Table 1, BQ-3). Apparently during approximately 100-fold concentration from BQ-6 to BQ-3, $\text{SiO}_2(\text{aq})$ decreases, indicating that it is removed from solution. It may be adsorbed onto mineral surfaces or it may be taken up to form authigenic silicate phases. Authigenic clay minerals may have formed in the muds adjacent the aquifer in quantities too small to be detected by the XRD studies. Alternatively, Si is incorporated into phases such as allophane (or very possibly alunite) which are either X-ray amorphous or are too fine grained to yield well defined XRD patterns.

Aqueous Al increases as Cl increases in the aquifer waters but in the brine Al is depleted relative to Cl; apparently it is removed from solution. Like

SiO₂, Al may be extracted from the brines to form fine grained clay minerals or X-ray amorphous Al-silicates. Detailed studies of the sheet silicates and fine grained fraction of the muds are required to determine, in detail, the nature of the silicate mineral-solution reactions.

DISCUSSION

The effect of calcite precipitation on the evolution of natural ground waters is well documented (GARRELS and MACKENZIE, 1967; HARDIE and EUGSTER, 1970; EUGSTER, 1970) and the influence of the formation of Mg-silicates has also been emphasized (DROUBI *et al.*, 1977). The influence of Mg-carbonates and particularly Ca-protodolomites are less well documented. Here, the authigenic salts and solution compositions from the Basque No. 2 Basin are presented to illustrate the role that Mg-carbonate minerals have on the evolution of the Mg-Na-SO₄ brines of the Basque Basin. Even in saline, Mg- and SO₄-rich brines, Mg-carbonates have precipitated in quantity and they probably precipitate and affect the evolution of other continental groundwaters and subsurface marine waters.

The evolution of other continental groundwaters can be classified into two great groups, those which precipitate protodolomite after calcite and those that precipitate gypsum after calcite. The dashed 'join' connecting the calcite corner to the calcite-protodolomite-gypsum-solution triple point (Fig. 8) separates the two groups. The Basque Basin waters are an example of the group which plot above the 'join' and SP-2 water (Table 1) from Spotted Lake Basin (Ossoyos, British Columbia, Canada) is a member of the second great group; the authigenic assemblage calcite plus gypsum (no protodolomite) is predicted to form after calcite precipitation and field studies reveal this zone in the Spotted Lake Basin. The zone separates the calcite zone from the Mg-sulphate zone (lake muds) and most importantly no protodolomite was found within the calcite + gypsum zone of Spotted Lake Basin.

Waters of the Basque Basin (Table 1) span the range of salinity of seawater and its evaporative concentrates, and like seawater, the Basque waters contain high proportions of Mg and SO₄. These waters apparently have maintained exchange equilibrium with carbonates regardless of salinity, Mg or SO₄ levels of the waters; consequently the thermodynamic model may serve to accurately predict the evolutionary path of seawater as it is concentrated in subsurface environments. Seawater is plotted on Fig. 9 as S.W. It falls in the calcite field

and upon concentration in the subsurface calcite is predicted to form either by precipitation, probably overgrowths, or through biological removal. The mechanism is inconsequential to the thermodynamic model and by either mechanism S.W. evolves away from the calcite corner as the solid is extracted from solution and CO₂ is evolved (Equation 1). Decaying organic material contribute HCO₃ to subsurface seawater, adding a vertical component to its evolutionary path on Fig. 9. Where significant HCO₃ is added to seawater, the path encounters the protodolomite field before the gypsum field, hence protodolomite may form before gypsum as a result of HCO₃ uptake and calcite (or aragonite) precipitation. Precipitation of gypsum follows, because the formation of the carbonates increases SO₄/HCO₃ values of the seawater concentrate. The model implies that Mg-calcite and Ca-protodolomite may form before, as, or after gypsum precipitates. Gypsum precipitation (BUTLER, 1969) or preferential storage of Mg by algae (GEBLELEIN and HOFFMAN, 1971) are two ways to increase Mg/Ca in seawater concentrates; precipitation of either carbonate also increases Mg/Ca values of seawater. The abundance of decaying organic matter may modify the sequence of authigenic salts formed.

CONCLUSIONS

Carbonate minerals, Mg-calcite, Ca-protodolomite and magnesite precipitate from the groundwaters of the Basque Basin. The precipitation of the carbonates and particularly Ca-protodolomite is pivotal to the evolution of the brines. Its formation results in depletion of the waters in HCO₃ relative to SO₄ so that evolved groundwaters are carbonate-depleted and sulphate-enriched. The result is precipitation of the very soluble sulphate salts epsomite and bloedite from the extremely concentrated brines. The precipitation of both calcite and protodolomite also have an important effect on the cations. Calcite precipitation depletes the groundwaters in Ca relative to the other major cations. Even the formation of protodolomite depletes the waters in Ca relative to Mg because the waters have Mg/Ca values much higher than unity when formation of protodolomite commences. Large amounts of protodolomite have formed over the last 6600 years (the life of the basin).

The studies of MUCCI *et al.* (1985) indicate that Mg-calcite overgrowths on calcite remain in exchange equilibrium with the solution over a wide range of levels of supersaturation (with respect to calcite). The data from the Basque Basin suggests

that exchange equilibrium is maintained between waters of the aquifer and Mg-calcite of varying compositions. The consequences are significant for they provide a means to model carbonate authigenesis in natural settings, including early and late diagenetic environments.

There is extensive interaction between the groundwaters and the sheet silicates of the basin muds. X-ray diffraction data demonstrate the effects to the silicates and the solution compositions confirm that Si and Al are removed from the groundwaters and/or brines. Potassium is also removed from the brines, and may be taken up by K-bearing silicates. Similarly some of the Mg lost from solutions may be taken up by the silicates. Comprehensive studies of the silicate phases are required to document and understand the nature and extent of these interactions.

Acknowledgements—I thank H. P. Eugster for encouraging me to study closed basins. The study of Mg-rich waters of closed basins was proposed by H. P. Eugster and L. A. Hardie and to both I am greatly indebted. T. Lowenstein and H. Machel read the manuscript and provided many improvements to the manuscript. The study was supported by two student grants from the Geological Society of America and by the National Sciences and Engineering Research Council of Canada.

REFERENCES

- ALDERMAN A. R. and SKINNER H. C. W. (1957) Dolomite sedimentation in the south-east of South Australia. *Amer. J. Sci.* **255**, 561–567.
- BARNES I. and O'NEIL J. R. (1971) Calcium-magnesium carbonate solid solutions from Holocene conglomerate cements and travertines in the Coast Range of California. *Geochim. Cosmochim. Acta* **32**, 415–432.
- BERNER R. A. (1975) The role of magnesium in the crystal growth of calcite and aragonite in seawater. *Geochim. Cosmochim. Acta* **39**, 489–504.
- BERNER R. A. (1978) Equilibrium, kinetics, and the precipitation of magnesian calcite from seawater. *Amer. J. Sci.* **278**, 1435–1477.
- BUTLER G. P. (1969) Modern evaporite deposition and geochemistry of coexisting brines, the sabkha, Trucial Coast, Arabian Gulf. *J. Sed. Petrol.* **39**, 70–89.
- CHRIST C. L. and HOSTETLER P. B. (1970) Studies in the system MgO-SiO₂-CO₂-H₂O (II): The activity product of magnesite. *Amer. J. Sci.* **268**, 439–453.
- DREVER J. I. (1971) Magnesium-iron replacement in clay minerals in anoxic marine sediments. *Science* **172**, 1334–1336.
- DROUBI A., FRITZ B., GAC Y. and TARDY Y. (1977) Prediction of the chemical evolution of natural waters during evaporation. *2nd Inter. Symp. Water-rock Interaction. Strasbourg*, Vol. II, 13–22.
- EUGSTER H. P. (1969) Inorganic bedded cherts from the Magadi area, Kenya. *Contrib. Mineral. Petrol.* **22**, 1–31.
- EUGSTER H. P. (1970) Chemistry and origin of the brines of Lake Magadi, Kenya. *Mineral. Soc. Amer. Spec. Pub.* **3**, 215–235.
- GAC J. Y., DROUBI A., FRITZ B. and TARDY Y. (1977) Geochemical behaviour of silica and magnesium during the evaporation of waters in Chad. *Chem. Geol.* **19**, 215–228.
- GARRELS R. M. and CHRIST C. L. (1965) *Solutions, Minerals and Equilibria*. 450 pp. Harper & Row.
- GARRELS R. M. and MACKENZIE F. T. (1967) Origin of the chemical compositions of some springs and lakes. In *Advances in Chemistry Series 67*, Washington, D.C., Amer. Chem. Soc., 222–242.
- GARRELS R. M. and WOLLAST R. (1978) Discussion of Thorstenson and Plummer, 1977. *Amer. J. Sci.* **278**, 1469–1474.
- GEBELEIN, C. D. and HOFFMAN, P. (1971) Algal origin of dolomite in interlaminated limestone-dolomite sedimentary rocks. In *Carbonate Cements. Studies in Geology*, **19** (ed. O. P. BRICKER), pp. 326. The Johns Hopkins University Press. Baltimore.
- GLOVER E. D. and PRAY L. C. (1969) High magnesium calcite and aragonite cementation within modern subtidal sediment grains. *Bermuda Biological Station for Research, Spec. Pub. 3, Carbonate Cements*, 46–57.
- GOLDSMITH J. R., GRAF D. L. and HEARD H. C. (1961) Lattice constants of the calcium magnesium carbonates. *Amer. Mineral.* **46**, 453–457.
- GOUDGE M. G. (1924) Magnesium sulphate in British Columbia. *Dept. of Mines No. 642*, Mines Branch, Canada.
- HARDIE L. A. (1968) The origin of the Recent non-marine evaporite deposit of Saline Valley, Inyo Co., California. *Geochim. Cosmochim. Acta* **32**, 1279–1301.
- HARDIE L. A. and EUGSTER H. P. (1970) The evolution of closed basin brines. *Mineral. Soc. Amer. Spec. Pub.* **3**, 273–290.
- HELGESON H. C. (1969) Thermodynamics of hydrothermal systems at elevated temperatures and pressures. *Amer. J. Sci.* **167**, 729–804.
- HELGESON H. C., DELANEY J. M., NESBITT H. W. and BIRD D. K. (1978) Summary and critique of the thermodynamic properties of rock-forming minerals. *Amer. J. Sci.* **278-A**, 1–229.
- JONES B. F. (1966) The hydrology and mineralogy of Deep Springs Lake. *U.S. Geol. Surv. Prof. Paper 502-A*.
- JONES B. F., EUGSTER H. P. and RETTIG S. L. (1977) Hydrochemistry of Lake Magadi basin, Kenya. *Geochim. Cosmochim. Acta* **41**, 53–72.
- LANGMUIR D. (1965) Stability of carbonates in the system MgO-CO₂-H₂O. *J. Geol.* **73**, 730–754.
- MUCCI A. and MORSE J. W. (1984) The solubility of calcite in seawater solutions of various magnesium concentration, $I_p = 0.697$ m at 25°C and one atmosphere total pressure. *Geochim. Cosmochim. Acta* **48**, 815–822.
- MUCCI A. and MORSE J. W. (1985) Auger spectroscopy determination of the surface-most adsorbed layer composition on aragonite, calcite, dolomite and magnesite in synthetic seawater. *Amer. J. Sci.* **285**, 306–317.
- MUCCI A., MORSE J. W. and KAMINSKY M. S. (1985) Auger spectroscopy analysis of magnesian calcite overgrowths precipitated from seawater and solutions of similar composition. *Amer. J. Sci.* **285**, 289–305.
- MULLER G., IRION G. and FORSTNER U. (1972) Formation and diagenesis of inorganic Ca-Mg carbonates in the Lacustrine environment. *Naturwissenschaften* **59**, 158–164.

Table A1. Activity coefficients* of Mg, Ca, HCO₃ and SO₄

Species	BQ-7	BQ-6	BQ-5	BQ-4	BQ-3	SP-2
Mg	0.13	0.13	0.12	0.084	0.10	0.37
Ca	0.18	0.18	0.17	0.127	0.16	0.44
HCO ₃	0.56	0.55	0.52	0.25	0.13	0.79
SO ₄	0.13	0.13	0.11	0.037	0.018	0.44
I.S.	0.30	0.29	0.36	1.74	3.25	0.027

* WATEQ (TRUEDELL and JONES, 1974) used to calculate the activity coefficients.

I.S. = stoichiometric ionic strength.

NESBITT H. W. (1975) The study of some mineral-solution interactions. *Ph D Thesis*, The Johns Hopkins University, Baltimore. 173p.

POWERS H. A. and WILCOX R. E. (1964) Volcanic ash from Mount Mazama (Crater Lake) and from Glacier Peak. *Science* **144**, 1334–1335.

ROBINSON R. A. and STOKES R. H. (1965) *Electrolyte Solutions*. 571pp. Butterworths.

ROSEN M. R. and WARREN J. K. (1988) Dolomite occurrence in the Coorong Region, South Australia (abstr.). *Amer. Assoc. Petrol. Geol. Bull.* **79**, 242.

ROSEN R. M., MISER D. E., STARCHER M. A. and WARREN J. K. (1989) Formation of dolomite in the Coorong region, South Australia. *Geochim. Cosmochim. Acta* **53**, 661–669.

SKINNER H. C. W. (1963) Precipitation of calcian dolomites and magnesian calcites in the southeast of Australia. *Amer. J. Sci.* **261**, 449–472.

THORSTENSON D. C. and PLUMMER L. N. (1977) Equilibrium criteria for two-component solids reacting with fixed composition in an aqueous phase—Example the magnesian calcites. *Amer. J. Sci.* **277**, 1203–1223.

THORSTENSON D. C. and PLUMMER N. L. (1978) Reply to comments on Thorstenson and Plummer, 1977. *Amer. J. Sci.* **278**, 1478–1488.

TOTH J. (1962) A theoretical analysis of groundwater flow in small drainage basins. *Third Canadian Hydrology Symp.*, Calgary, 75–96.

TRUEDELL A. H. and JONES B. F. (1974) WATEQ, a computer program for calculating chemical equilibria of natural waters. *J. Res. U.S. Geol. Surv.* **2**, 233–248.

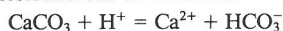
VON DER BORSCH C. C. (1965) The distribution and Preliminary geochemistry of modern carbonate sediments of the Coorong area, South Australia. *Geochim. Cosmochim. Acta* **29**, 781–799.

WOOD J. R. (1975) Thermodynamics of brine-salt equilibria, I. The systems NaCl-KCl-MgCl₂-CaCl₂-H₂O at 25°C. *Geochim. Cosmochim. Acta* **39**, 1147–1163.

APPENDIX

Experimental and thermochemical data are used to determine phase relations in the system CaCO₃-MgCO₃-CaSO₄-MgSO₄. All phase relations are determined for 1 bar total pressure and 25°C and a pH of 7.0, which is typical of the Basque Lake #2 Basin waters. The diagram is constructed for the Basque Basin waters.

Calcite dissolution can be written as:



and the mass action equation is:

$$10^{1.95} = [\text{Ca}^{2+}][\text{HCO}_3^-]/([\text{H}^+][\text{Cc}]). \quad (1A)$$

The mass action equation for gypsum dissolution is:

$$10^{-4.4} = [\text{Ca}^{2+}][\text{SO}_4^{2-}][\text{H}_2\text{O}]^2/[\text{Gyp}]. \quad (2A)$$

Square brackets denote activities, Cc and Gyp represent the respective CaCO₃ and CaSO₄·H₂O components in calcite and gypsum phases. Activities of Cc and Gyp are taken as 1.0. The equilibrium constants for equations (1A) and (2A) are taken from HELGESON (1969) and HARDIE (1968). For a solution equilibrated with respect to these phases:

$$10^{-6.35} = [\text{SO}_4^{2-}][\text{H}^+]/[\text{HCO}_3^-]. \quad (3A)$$

The substitution of activity coefficients and molalities for activities in Equation (3A), and taking logarithms yields:

$$-6.35 + \text{pH} = \log \{ \gamma(\text{SO}_4)/\gamma(\text{HCO}_3) \} \\ + \log \{ m(\text{SO}_4)/m(\text{HCO}_3) \} \quad (4A)$$

where γ denotes activity coefficient and m denotes molality. For near-neutral solutions (pH = 7), as for the Basque waters, equation (4A) gives:

$$0.65 + \log \{ \gamma(\text{SO}_4)/\gamma(\text{HCO}_3) \} \\ = \log \{ m(\text{SO}_4)/m(\text{HCO}_3) \} \quad (5A)$$

Since SO₄ is doubly charged its activity coefficient is lower than that of HCO₃ in dilute solutions where complex ions are insignificant (GARRELS and CHRIST, 1965, p. 63 and p. 104). For solutions of ionic strength equal 0.1, the extended Debye-Huckel equation yields activity coefficients of 0.77 and 0.36 for HCO₃ and SO₄. These values are substituted into Equation (4A);

$$9.7 \approx (\text{SO}_4^{2-})/(\text{HCO}_3^-) \quad (6A)$$

hence,

$$0.91 \approx (\text{SO}_4^{2-})/(\text{HCO}_3^- + \text{SO}_4^{2-}). \quad (7A)$$

Table (A1) lists the stoichiometric activity coefficients for SO₄ and HCO₃ in the Basque Lake #2 Basin waters (calculated using WATEQ, TRUEDELL and JONES, 1974). If the activity coefficients for SO₄ and CO₃ are substituted into Equation (3A), the value of 0.91 represents a maximum for the Basque waters. The proportion of sulphate in solution therefore ranges from approximately 0.9 to 1 for the Basque Lake and Spotted Lake Basin waters and for most other natural waters. Only in solutions where the percentage of HCO₃ is appreciably more complexed than the percentage of SO₄ will the value of Equation (7A) be less than 0.9. The situation is unlikely in natural solutions, hence the calcite-gypsum-solution eutectic curve plots very close to the CaSO₄-MgSO₄ boundary of Fig. 9, regardless of the composition of the solutions.

The mass action equation for epsomite-solution equilibrium is:

$$10^{-2.13} = [\text{Mg}^{2+}][\text{SO}_4^{2-}][\text{H}_2\text{O}]^7/[\text{Ep}], \quad (8A)$$

where Ep is the $\text{MgSO}_4 \times 7\text{H}_2\text{O}$ component of epsomite. The equilibrium constant is taken from WOOD (1975) and activities of H_2O in solutions equilibrated with epsomite are taken from ROBINSON and STOKES (1965). A solution equilibrated with respect to gypsum and epsomite yields:

$$10^{2.2} = [\text{Mg}^{2+}]/[\text{Ca}^{2+}]. \quad (9A)$$

In dilute solutions where Ca and Mg complexes are unimportant, and in the Basque waters (Table A1), activity coefficients of Ca and Mg do not differ greatly. By analogy with the derivation of Equation (7A):

$$1.0 \approx (\text{Mg}^{2+})/(\text{Mg}^{2+} + \text{Ca}^{2+}), \quad (10A)$$

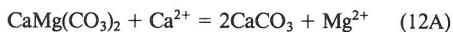
where again the rounded brackets denote molalities.

Stabilities of the Mg-carbonates are difficult to assess. HELGESON *et al.* (1978) note that the experimentally determined activity products for the reaction:



range from $10^{-16.4}$ to $10^{-19.3}$ and analysis of hydrothermal experimental results yields a range between $10^{-16.5}$ and $10^{-18.1}$. The value applicable to a sample is dependent upon the degree of order of the sample. Protodolomite from the Basque Basin displays no ordering peaks and is considered to be completely disordered; consequently an equilibrium constant of $10^{-16.4}$ is selected to represent the Basque Lake Basin protodolomites.

For calcite-protodolomite equilibrium:



Addition of Equations (1A) and (11A) and the logarithms of the equilibrium constants yields the mass action equation:

$$2.51 = [\text{Mg}][\text{Cc}]/([\text{Ca}][\text{Pr}]), \quad (13A)$$

hence,

$$0.72 = [\text{Mg}]/([\text{Mg}] + [\text{Ca}]) \quad (14A)$$

If the activity coefficients of Mg and Ca are the same (not necessarily 1.0), then the molar proportions are:

$$0.72 = (\text{Mg})/\{(\text{Mg}) + (\text{Ca})\}, \quad (15A)$$

which represents the value for the calcite-protodolomite-solution stability field boundary (Fig. 9). The boundary is applicable to all waters where there is no appreciable complexing of Mg or Ca, and where the Debye-Huckel equation is accurate (solutions of ionic strength up to approximately 0.1). In waters containing appreciable SO_4 , such as seawater and the Basque Basin waters, Mg is complexed by SO_4 in preference to Ca, thus the value for Equation (15A) is greater than 0.72. The solution from BQ-7, for example, yields a value of 0.93 (and 0.907 for Equation 14A). Protodolomite is present at BQ-7, hence protodolomite saturation and precipitation has already occurred when the value 0.93 has been achieved for $(\text{Mg})/\{(\text{Mg}) + (\text{Ca})\}$. The calcite-protodolomite equilibrium boundary applicable to the Basque Basin waters therefore is constrained between values of 0.72 and 0.93. The equilibrium value (Equation 15A) is likely to be closer to 0.93 than 0.72 for two reasons. BQ-7 is close to the site where protodolomite is first detected (BQ-12), thus the solutions are unlikely to have evolved greatly between BQ-12 and BQ-7. Secondly, the value of 0.72 is calculated using stoichiometric compositions for calcite and protodolomite. $\text{Mg}/(\text{Mg} + \text{Ca})$ of 0.87 (Equation 15A) is taken as representative of equilibrium among calcite, protodolomite and solution. The stability field boundary is plotted at this value on Fig. 9. The value is between the two extremes 0.72 and 0.93, but is closer to BQ-7 water because the data from BQ-7 probably is close to the equilibrium value.

LANGMUIR (1965) notes that experimentally determined activity products for magnesite vary by almost three orders of magnitude. CHRIST and HOSTETLER (1970) indicate that the activity product of magnesite is greater than $10^{-8.2}$ but an activity quotient as high as 10^{-5} may be required to precipitate the phase. The extreme value of 10^{-5} is taken here as activity quotient required for magnesite precipitation. The equilibrium constant for protodolomite ($10^{-16.4}$) is used with the activity quotient for magnesite to calculate the magnesite-protodolomite-solution field boundary. The result is a very small stability field for magnesite (Fig. 9). It has been expanded somewhat in Fig. 9 to illustrate the geometric relations among the different fields.

The magnesite activity quotient and equilibrium constant for epsomite are used to calculate the magnesite-epsomite-solution field boundary (lower right-hand corner of Fig. 9). Equilibrium constants for the salts of Fig. 9 are used to calculate all field boundaries of Fig. 9. Assumptions and calculations are identical to those presented in the previous paragraphs.

